

Nonpolar optical scattering of positronium in magnesium fluoride

I. V. Bondarev,^{1,2,*} Y. Nagai,³ M. Kakimoto,⁴ and T. Hyodo⁵

¹*Institute for Nuclear Problems, Belarusian State University, Bobruiskaya Str. 11, 220050 Minsk, Belarus*

²*Laboratoire d'Annecy-le-Vieux de Physique des Particules, BP 110 74941 Annecy-le-Vieux Cédex, France*

³*Institute for Materials Research, Tohoku University, Oarai, Ibaraki 311-1313, Japan*

⁴*Communication and Information System Laboratories, R & D Center, Toshiba, 1 Komukai, Toshiba-Cho, Kawasaki, Kanagawa 212-8582, Japan*

⁵*Institute of Physics, Graduate School of Arts and Sciences, University of Tokyo, 3-8-1 Komaba, Meguro-ku, Tokyo 153-8902, Japan*

(Received 15 March 2005; published 14 July 2005)

We report the results of the analysis of the temperature broadening of the momentum distribution of delocalized positronium (Ps) in magnesium fluoride in terms of the optical deformation-potential scattering model (long-wavelength optical phonons). The Ps optical deformation-potential coupling constant D_o in MgF_2 has been determined to be $(1.8 \pm 0.3) \times 10^9$ eV/cm. We also show that the Ps momentum distribution is sensitive to second-order phase transitions in those crystals where optical deformation-potential scattering is allowed in one and forbidden in another crystalline phase.

DOI: [10.1103/PhysRevB.72.012303](https://doi.org/10.1103/PhysRevB.72.012303)

PACS number(s): 78.70.Bj, 71.38.-k, 71.60.+z

Magnesium fluoride, which is commonly used for optical elements of extreme ruggedness and durability in both the infrared and ultraviolet (see, e.g., Ref. 1), has recently been proven to be a good host material for three-dimensional atom optical lithography on the nanometer scale.^{2,3} In this technique, the resonance atom-light interaction of dopant atoms is utilized to structure their positions inside the host MgF_2 matrix and thus to engineer electronic and photonic features (e.g., a photonic band) of a composite solid. In such nanostructural applications, it is important to understand vibrational properties of a host material because the vibrations disturb electronic and photonic bands of the nanocomposite via deformation potentials. The latter are caused by acoustic and optical strains created by acoustic and optical vibrational modes, respectively. These strains influence the particle in its band in two distinct ways (see, e.g., Refs. 4 and 5). In the first way, short-range disturbances of the periodic potential cause practically instantaneous changes in energy, and these are the ones quantified by deformation-potentials and referred to as deformation-potential scattering (acoustic and nonpolar optical, respectively). In the second way, the distortion of the lattice may destroy local electric neutrality, and produce electric polarization and associated macroscopic comparatively long-range electric fields to which the particle responds. Disturbance of the particle's motion by this effect is referred to as piezoelectric scattering, if associated with acoustic modes, and polar optical scattering, if associated with optical modes. Because of its electric neutrality, the positronium atom [$\text{Ps}=(e^+e^-)$] is less sensitive to the latter two,⁶ thus providing a unique opportunity to study short-range deformation-potential interactions only.

Physical nature of Ps states in crystalline dielectrics has been of continued interest for more than three decades⁶⁻¹⁸ ever since Brandt *et al.* first identified the delocalized Ps state in the Angular Correlation of Annihilation Radiation (ACAR) spectrum of the single crystal of $\alpha\text{-SiO}_2$.⁷ The formation of Bloch-type Ps is confirmed by observing very narrow peaks (the central peak and satellite peaks appearing at

the momentum corresponding to the reciprocal lattice vectors of the sample crystal) in the ACAR spectra resulting from the 2γ -decay of Ps and representing its momentum distribution in a crystal. Positronium in the MgF_2 and $\alpha\text{-SiO}_2$ crystals is known to form a delocalized state in a wide temperature range from ~ 10 K up to ~ 700 K.¹³ This is contrast to the case of alkali halides where, as temperature increases, the central Ps peak becomes drastically wider and the satellite peaks disappear, indicating the localization of Ps.¹⁰ Such an effect of a thermally activated self-localization (self-trapping) of Ps was observed in a number of dielectric crystals and was studied theoretically in Refs. 11 and 12 in terms of the interaction of Ps with the field of a short-range acoustic deformation-potential (long-wavelength longitudinal acoustic phonons).

In MgF_2 , the central and satellite positronium ACAR peaks are observed to be remarkably broadened above 200 K, but not so drastically as in alkali halides. Although attempts have been made,¹³ this extraordinary broadening has not been explained in terms of Ps acoustic deformation-potential scattering alone, whereas such an explanation was a success for $\alpha\text{-SiO}_2$.⁸ An effect appeared as if there were an additional scattering mechanism activated at temperatures above 200 K which renormalized the acoustic deformation-potential coupling constant so that it increased by a factor of approximately 2 in the narrow temperature range 200–355 K. In Ref. 13, an extraordinary broadening of the Ps peaks in MgF_2 was interpreted by involving short-wavelength acoustic phonon scattering in terms of the Umklapp mechanism. However, later on this mechanism was shown not to be the case up to $T \sim 10^4$ K,¹⁴ being ruled out by the Boltzmann energy distribution of delocalized Ps atoms.

In the present Brief Report, we report the results of the analysis of the temperature broadening of the momentum distribution of delocalized Ps in MgF_2 in terms of the optical deformation-potential scattering model (long-wavelength optical phonons). Such a nonpolar optical scattering mechanism is known to be the case in crystals with two and more

atoms per elementary cell at elevated temperatures when a corresponding coupling constant is nonzero because of the selection rules dictated by local symmetry restrictions.^{4,5} We obtain the numerical value of the optical deformation-potential coupling constant in MgF₂ for the first time and discuss possible applications of delocalized Ps states for the study of symmetry dependent structural properties of crystal-line dielectrics.

In terms of the Green functions formalism,¹⁹ the linear projection experimentally measured of the momentum distribution (1D-ACAR spectrum) of the thermalized Ps atom interacting with phonons at finite temperatures is given by¹³

$$N_{1D}(p_x) \sim \int_{-\infty}^{\infty} dp_z \int_{-\infty}^{\infty} dp_y \int_0^{\infty} d\omega e^{-\omega/k_B T} \times \frac{\Gamma_{\mathbf{k}}(\omega)}{(\omega - \mathbf{p}^2/2M^*)^2 + \Gamma_{\mathbf{k}}^2(\omega)}, \quad (1)$$

where the exponential factor stands for the Boltzmann statistics because there is at most only one Ps atom at a time under usual experimental conditions. The nonexponential factor represents the so-called spectral density function in its explicit form with $\Gamma_{\mathbf{k}}(\omega)$ being the imaginary self-energy of Ps with the quasimomentum $\mathbf{k}=\mathbf{p}/\hbar$. In the weak phonon coupling regime (delocalized Ps, see Ref. 11), $\Gamma_{\mathbf{k}}(\omega)$ is usually written to the leading (second) order approximation in the Ps interaction with a phonon field,

$$\Gamma_{\mathbf{k}}(\omega) = \pi \sum_{\mathbf{q}} |V_{\mathbf{q}}|^2 \{ n(\omega_{\mathbf{q}}) \delta(\omega - E_{\mathbf{k}+\mathbf{q}} + \hbar\omega_{\mathbf{q}}) + [n(\omega_{\mathbf{q}}) + 1] \delta(\omega - E_{\mathbf{k}+\mathbf{q}} - \hbar\omega_{\mathbf{q}}) \}, \quad (2)$$

where $V_{\mathbf{q}}$ is the Ps-phonon interaction matrix element, $E_{\mathbf{k}} = \hbar^2 \mathbf{k}^2 / 2M^*$ is the energy of Ps with the band mass M^* , $n(\omega_{\mathbf{q}}) = [\exp(\hbar\omega_{\mathbf{q}}/k_B T) - 1]^{-1}$ is the equilibrium phonon distribution function, and $\omega_{\mathbf{q}}$ is the frequency of the phonon with the wave vector \mathbf{q} . With allowance made for acoustic deformation-potential scattering alone, Eq. (2) transforms to^{13,14}

$$\Gamma_{\mathbf{k}}(\omega) = \Gamma_{\mathbf{k}}^{(a)}(\omega) = \frac{E_d^2 M^{*3/2} k_B T}{\sqrt{2} \pi \hbar^3 u^2 \rho} \sqrt{\omega}, \quad (3)$$

where E_d is the coupling constant of Ps to the deformation-potential produced by long-wavelength longitudinal acoustic vibrational modes, u and ρ are the sound velocity and density of a crystal, respectively.

Magnesium fluoride is an optically transparent insulator which crystallizes with the rutile structure of the point group D_{4h} .²⁰ A group character analysis shows that this material should exhibit nine optical infrared vibrational modes in total²¹—three nondegenerate longitudinal and three doubly degenerate transverse modes of symmetry E_u plus one longitudinal and two nondegenerate transverse modes of symmetry A_{2u} . In our analysis, we apply an isotropic approximation in considering nonpolar optical phonon scattering of Ps. Within this approximation the nonpolar optical contribution to the imaginary self-energy (2) is of the form¹⁴

$$\Gamma_{\mathbf{k}}^{(o)}(\omega) = \frac{D_o^2 M^{*3/2} \sqrt{\omega}}{2\sqrt{2} \pi \hbar^2 \rho \omega_o} \left\{ n(\omega_o) \sqrt{1 + \frac{\hbar\omega_o}{\omega}} + [n(\omega_o) + 1] \times \theta \left(1 - \frac{\hbar\omega_o}{\omega} \right) \sqrt{1 - \frac{\hbar\omega_o}{\omega}} \right\}, \quad (4)$$

where D_o is the coupling constant of Ps to the deformation-potential produced by long-wavelength optical vibrations of averaged frequency ω_o with the phonon distribution function $n(\omega_o) = [\exp(\hbar\omega_o/k_B T) - 1]^{-1}$, and $\theta(x)$ is the unit-step function. The total imaginary self-energy accounting for two types of Ps-phonon scattering (acoustic and nonpolar optical) is then written as

$$\Gamma_{\mathbf{k}}(\omega) = \Gamma_{\mathbf{k}}^{(a)}(\omega) + \Gamma_{\mathbf{k}}^{(o)}(\omega) = \frac{\tilde{E}_d^2(\omega) M^{*3/2} k_B T}{\sqrt{2} \pi \hbar^3 u^2 \rho} \sqrt{\omega} \quad (5)$$

with

$$\tilde{E}_d(\omega) = \left\{ E_d^2 + \frac{\hbar u^2 D_o^2}{2k_B T \omega_o} \left[n(\omega_o) \sqrt{1 + \frac{\hbar\omega_o}{\omega}} + [n(\omega_o) + 1] \times \theta \left(1 - \frac{\hbar\omega_o}{\omega} \right) \sqrt{1 - \frac{\hbar\omega_o}{\omega}} \right] \right\}^{1/2} \quad (6)$$

representing the “effective” deformation-potential coupling constant with nonpolar optical scattering taken into account. In view of an obvious fact that frequencies $\omega \sim k_B T$ only contribute to the Ps momentum distribution (1), one may approximate $\tilde{E}_d(\omega) \approx \tilde{E}_d(k_B T)$ and then \tilde{E}_d is easily seen to increase in its value from E_d (for $T \ll \hbar\omega_o/k_B$) to $\tilde{E}_d = \sqrt{E_d^2 + (u D_o / \omega_o)^2}$ (for $T \gg \hbar\omega_o/k_B$). This explains the increase of the Ps-phonon coupling constant and corresponding extraordinary broadening of the Ps momentum distribution in MgF₂ at elevated temperatures reported earlier in Ref. 13.

Inserting Eqs. (5) and (6) into Eq. (1) and performing the integration over p_y and p_z , one obtains in dimensionless variables

$$N_{1D}(p_x) \sim \int_0^{\infty} d\xi \xi e^{-\xi^2} \left\{ \arctan \left[\frac{\xi^2 - p_x^2 / (2M^* k_B T)}{\Gamma^{(a)}(\xi) + \Gamma^{(o)}(\xi)} \right] + \frac{\pi}{2} \right\} \quad (7)$$

with $\xi = \sqrt{\hbar\omega/k_B T}$ and $\Gamma^{(a),(o)}(\xi) = \Gamma_{\mathbf{k}}^{(a),(o)}(\omega) / k_B T$. We use Eq. (7) to observe how important nonpolar optical scattering is in MgF₂ at different temperatures. To this end we define a mean-square deviation function

$$S = \sum_i \left\{ \frac{I_{1D}[p_x^{(i)}]}{I_{1D}(0)} - \frac{\bar{N}_{1D}[p_x^{(i)}]}{\bar{N}_{1D}(0)} \right\}^2, \quad (8)$$

where $\{I_{1D}[p_x^{(i)}]\}_{i=1}^N$ is a set of intensities representing a 1D-ACAR spectrum measured at fixed temperature (a complete description of experimental measurements is found elsewhere¹³), N is the number of data points, and \bar{N}_{1D} is the momentum distribution (7) convoluted with an experimental resolution function which was the Gaussian function of FWHM = $0.297 \times 10^{-3} mc$ (m is the free electron mass, c is the speed of light). We then plot Eq. (8) with $E_d = 7.6$ eV and

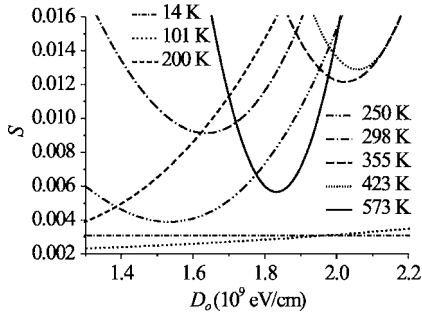


FIG. 1. The function $S(D_o)$ at different temperatures.

$M^* = 1.1 \times 2m$ (Ref. 13) as a function of the optical deformation-potential coupling constant D_o at those temperatures at which the ACAR measurements were done. Other material parameters were fixed as follows: $\omega_o = 7.7 \times 10^{13}$ rad/s, $u = 7 \times 10^5$ cm/s (averaged over directions and phonon polarizations; from Refs. 21 and 22, respectively), $\rho = 3.13$ g/cm³.²⁰

The results are presented in Fig. 1. At $T \leq 200$ K, the function $S(D_o)$ is either a constant (at very low $T \sim 10$ K) or tends to its minimal value at $D_o \sim 0$, thus indicating the absence of nonpolar optical scattering at these temperatures. This is clear as optical vibrational degrees of freedom are frozen at temperatures below $\hbar\omega_o/2k_B$ (the optical zero-point vibration energy divided by k_B) which is estimated to be ~ 300 K for MgF₂. For all $T \geq 250$ K, clear minima are seen in $S(D_o)$ at approximately the same value of the optical deformation-potential coupling constant $\sim 1.8 \times 10^9$ eV/cm. This indicates that nonpolar optical scattering comes into play above 250 K and starts broadening the Ps momentum distribution which was initially broadened by acoustic deformation-potential scattering. From this analysis we obtain $D_o = (1.8 \pm 0.3) \times 10^9$ eV/cm for the delocalized Ps atom in MgF₂. Figure 2 shows the theoretical curves $\bar{N}_{1D}(p_x)/\bar{N}_{1D}(0)$ (solid lines) plotted for this value of D_o along with the normalized central peaks of the experimental 1D-ACAR spectra at different temperatures. The dashed lines above 200 K represent the theoretical momentum distribution with only acoustic deformation-potential scattering taken into account. The experimental spectra are clearly seen to be very nicely reproduced theoretically at all the temperatures in terms of the Ps nonpolar optical scattering model.

A similar effect of an optical deformation-potential was not observed in α -SiO₂ (crystalline quartz) where the temperature broadening of the central and satellite 1D-ACAR peaks of delocalized Ps was explained in terms of acoustic deformation-potential scattering alone throughout the entire temperature range 88–701 K.^{8,13} In long-wavelength optical vibrations, one set of atoms moves as a body against the second set of atoms of the same elementary cell. This changes the particle's energy by an amount $\sim \mathbf{D}_o \cdot \mathbf{u}$ with \mathbf{u} being the relative displacement of the two atomic sets and \mathbf{D}_o representing the vectorial optical deformation-potential constant ($|\mathbf{D}_o| = D_o$) which is nothing but the matrix element of a perturbation operator (i.e., the variation of the rigid-lattice potential due to optical vibrations) taken over Bloch wave functions of the particle in the neighborhood of its energy

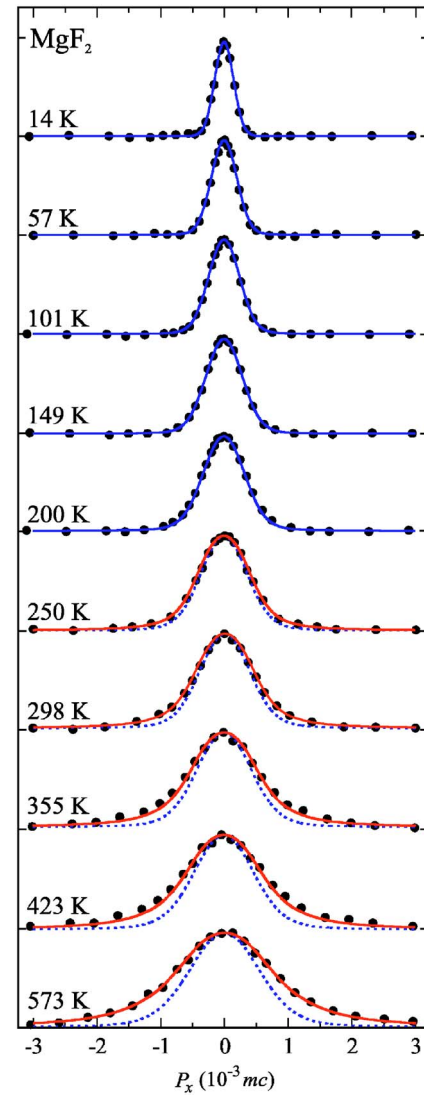


FIG. 2. (Color online) The central peaks of the 1D-ACAR spectra of Ps in MgF₂ at different temperatures as calculated from Eq. (7) convoluted with an experimental resolution function (see text for explanations).

band minimum.^{4,5} Since we deal with the Ps atom having a parabolic band with its minimum in the center of the Brillouin zone (Γ -valley), for this additional energy to be non-zero, \mathbf{D}_o and \mathbf{u} must transform according to equal-dimension irreducible representations of the point symmetry group of the Γ -point of the Brillouin zone. In terms of such a symmetry analysis,⁵ optical deformation-potential scattering is allowed in the Γ -valley of the MgF₂ lattice (point group D_{4h}) and forbidden in the Γ -valley of the α -SiO₂ lattice (point group D_3 with the C_3 -axis being a screw axis). However, crystalline quartz is known to undergo the second-order structural phase transition from α - to β -phase above 846 K,²⁰ where its local symmetry changes from D_3 to D_6 . The latter one is isomorphic (thus having the same set of group representations and the same selection rules for deformation-potential scattering in the Γ -valley) to the C_{6v} local symmetry of wurtzite-type crystals which was analyzed in detail in Ref. 5 and shown to allow optical deformation-

potential scattering in the Γ -valley. Thus, Ps nonpolar optical phonon scattering must manifest itself in β -SiO₂ by drastically broadening the Ps 1D-ACAR peaks above 846 K.¹⁸

In summary, temperature broadening of the momentum distribution of delocalized Ps in magnesium fluoride has been analyzed in terms of the optical deformation-potential scattering model. The Ps optical deformation-potential coupling constant D_o in MgF₂ has been determined for the first time to be $(1.8 \pm 0.3) \times 10^9$ eV/cm. In view of the fact that the lowest positron band in alkali halides is not considerably different from the conduction band of the electron,²³ the positron optical deformation-potential coupling constant may be thought of being approximately equal to that of the electron. Then, one obtains an estimate of 9×10^8 eV/cm for the electron optical deformation-potential coupling constant in MgF₂. This agrees with typical values usually given in the literature for other materials (see, e.g., Ref. 24). We have

also shown that, as short-range deformation-potentials are essentially symmetry dependent, Ps may be able to sense symmetry dependent structural properties of dielectric crystals. In particular, high-temperature second-order phase transitions, where the local symmetry of a crystal lattice changes but the crystal structure remains, may be identified via jumps in the temperature dependencies of HWHMs of Ps peaks measured in ACAR-experiments in those dielectric crystals where optical deformation-potential scattering is allowed in one and forbidden in another crystalline phase.

One of the authors (I.V.B.) would like to acknowledge the financial support from the University of Savoie (France) within a Visiting Professorship Program. I.V.B. would also like to thank I.D. Feranchuk, L.V. Keldysh, L.I. Komarov, and V.N. Kushnir for useful discussions.

*Corresponding author. E-mail: bondarev@tut.by

¹M. Blanc and A. Malherbe, *J. Opt.* **8**, 195 (1977).

²Th. Schulze, T. Mütther, D. Jürgens, B. Brezger, M. K. Oberthaler, T. Pfau, and J. Mlynek, *Appl. Phys. Lett.* **78**, 1781 (2001).

³T. Mütther, Th. Schulze, D. Jürgens, M. K. Oberthaler, and J. Mlynek, *Microelectron. Eng.* **57–58**, 857 (2001).

⁴B. K. Ridley, *Quantum Processes in Semiconductors* (Clarendon, Oxford, 1993).

⁵G. L. Bir and G. E. Pikus, *Symmetry and Deformation Effects in Semiconductors* (Nauka, Moscow, 1972) [Wiley, New York, 1975].

⁶O. V. Boev and K. P. Aref'ev, *Phys. Status Solidi B* **125**, 619 (1984).

⁷W. Brandt, G. Coussot, and R. Paulin, *Phys. Rev. Lett.* **23**, 522 (1969).

⁸H. Ikari, *J. Phys. Soc. Jpn.* **46**, 97 (1979).

⁹A. Dupasquier, in *Positron Solid State Physics*, edited by W. Brandt and A. Dupasquier (North-Holland, Amsterdam, 1983), p. 510, and references therein.

¹⁰J. Kasai, T. Hyodo, and K. Fujiwara, *J. Phys. Soc. Jpn.* **57**, 329 (1988), and references therein.

¹¹I. V. Bondarev and T. Hyodo, *Phys. Rev. B* **57**, 11341 (1998).

¹²I. V. Bondarev, *Phys. Rev. B* **58**, 12011 (1998).

¹³Y. Nagai, M. Kakimoto, T. Hyodo, K. Fujiwara, H. Ikari, M. Eldrup, and A. T. Stewart, *Phys. Rev. B* **62**, 5531 (2000).

¹⁴I. V. Bondarev, *Phys. Lett. A* **291/1**, 39 (2001).

¹⁵Th. Gessmann, J. Major, A. Seeger, and J. Ehmann, *Philos. Mag. B* **81**, 771 (2001).

¹⁶H. Saito and T. Hyodo, *Phys. Rev. Lett.* **90**, 193401 (2003).

¹⁷N. Suzuki, H. Saito, Y. Nagai, T. Hyodo, H. Murakami, M. Sano, I. V. Bondarev, and S. A. Kuten, *Phys. Rev. B* **67**, 073104 (2003); *Mater. Sci. Forum* **445–446**, 410 (2004).

¹⁸I. V. Bondarev, *Nucl. Instrum. Methods Phys. Res. B* **221**, 230 (2004).

¹⁹G. D. Mahan, *Many-Particle Physics* (Plenum, New York, 1993).

²⁰*American Institute of Physics Handbook*, edited by D. E. Gray (McGraw-Hill, New York, 1972).

²¹A. S. Barker, Jr., *Phys. Rev.* **136**, A1290 (1964).

²²K. S. Aleksandrov, L. A. Shabanova, and V. I. Zinenko, *Phys. Status Solidi* **33**, K1 (1969).

²³A. B. Kunz and J. Waber, *Solid State Commun.* **39**, 831 (1981).

²⁴M. Neuberger, *Handbook of Electronic Materials* (Plenum, New York, 1971).